

Investigation of the Projector Properties of the Magnetic lenses Using Analytical Function

A. H.H. Al-Batat, M. J. Yaseen, M.M. Majeed*

Department of Physics, College of Education, University of Mustansiriyah

*Department of Biomedical, Al-Khawarizmi College of Engineering, Baghdad University

Received in Sept. 29 , 2010

Accepted in Feb. 8 , 2011

Abstract

A computational investigation has been carried out to describe synthesis optimization procedure of magnetic lenses. The research is concentrated on the determination of the inverse design of the symmetrical double polepiece magnetic lenses whose magnetic field distribution is already defined. Magnetic lenses field model well known in electron optics have been used as the axial magnetic field distribution. This field has been studied when the halfwidth is variable and the maximum magnetic flux density is kept constant. The importance of this research lies in the possibility of using the present synthesis optimization procedure for finding the polepieces design of symmetrical double polepiece magnetic lenses which have the best projector focal properties.

Key word: Electron optics, magnetic electron lenses, optimization of magnetic lenses, inverse design of magnetic lens.

Introduction

In electron optics, the synthesis procedure of electron lenses optimization is based on the fact that, the first-order properties and aberrations of any imaging magnetic field can be calculated by using mathematical functions to approximate the magnetic field several good mathematical functions exist for assigning the magnetic field distribution such as Gaussian model, Exponential model, Cosine model etc. It is important to note that, the values of optical properties, aberrations and polepiece shape depend on the mathematical distribution of field function i.e. the optimum design of magnetic lenses depend on the optimization parameters of proposed formula to represent the optimum axial magnetic field distribution [1].

The Mathematical Model

Depending on the similarity between the curve shapes of the axial magnetic scalar potential distribution and the hyperbolic tangent function, this following function can be used for approximating the axial magnetic scalar potential distribution V_z given by [2].

$$V_z(z)=\alpha \tanh(Z/\beta) \quad (1)$$

$Z_S \leq Z \leq Z_E$ along the axial length of the lens, where Z_S and Z_E are the terminals of the axial coordinate, here $(\alpha=W.B_{max} / 2\mu_0)$ and $(\beta=W / 2)$. Where μ_0 is the space permeability and equal $4\pi \times 10^{-7} \text{ H.m}^{-1}$, W is the halfwidth of the field distribution, B_{max} is the maximum magnetic flux density. W and B_{max} represent two optimization parameters.

For symmetrical charged particle lens, the magnetic field and its axial potential distribution would be symmetric about the mid plane. Therefore, the following constraints can be studied:

1. $B(z)=B(-z), V(z)=V(-z)$
2. $|Z_S|=Z_E$

accordingly the lens length can be expressed as $L=2Z_E$ or $L=2Z_S$.

In the synthesis technique, symmetric conditions depend on the procedure taken under considerations for a electron lens design. However, these conditions depend on the target function to be analyzed. For more details see [3,4,5,6].

For iron-free region the axial magnetic flux density distribution along the optical axis can be determined with the aid of the following eq. [2] :

$$B_z(z) = -\mu_0 \frac{dV_z}{dz} \tag{2}$$

Therefore, in the present work the axial magnetic field of the lens can be approximated by the following eq. :

$$B_z(z)=B_{max}\text{sech}^2(2.270(Z/W)) \tag{3}$$

It can be seen that the target function represented in eq. 3 has three main control parameters B_{max} , the maximum magnetic flux density, the halfwidth of the field distribution W , and the lens length $L(=Z_E - Z_S)$. The present investigation concerns with the more effective design parameter which is the halfwidth, while the other two parameters B_{max} and L are kept constant at 1T and 40mm.

Polepiece Reconstruction

To determine the lens potential, the region of its axial extension is divided into (n-1) subintervals where n represents the points of the field along the z-axis. By numerical analysis the axial magnetic flux density distribution B_z is represented by a cubic spline function in each subinterval [3]. By using the eq. 2 and with the aid of the cubic spline technique, the axial magnetic scalar potential may be given by:

$$V_{Z(k+1)} = V_{Zk} - G_k \tag{4}$$

where:

$$G_k = \mu_0 \left[B_k h_k + B_k \left(\frac{h_k}{2} \right)^2 + B_k \left(\frac{h_k}{2} \right)^3 \left(\frac{B_{k+1}}{3} \right) \left(\frac{h_k}{2} \right)^3 \right] \tag{5}$$

Here $h_k=z_{k+1} - z_k$; it represents the width of each subinterval. When the lens is symmetrical $V_Z(n)=-V_{Z(1)}=0.5 \text{ NI}$.

Consider the magnetic field model given in eq. 3. The magnetic field distribution is determined under symmetric conditions along the lens optical axis. Since the lens is symmetric, then the absolute value of the potential at the lens terminals are equal in magnitude (see fig. 1). This indicates that the area under the condenser and objective fields are equal. At the plane where $z=0$ the potential is zero as shown in fig. (1). The symmetrical lens is achieved by maintaining this plane and keeping the condenser field on its left-hand side equivalent to the objective field on the right-hand side.

By using the analytical solution of Laplace's equation, the shape of the polepiece that would produce the desired field can be determined. For axially symmetric systems the electrostatic or magnetic scalar potential $V(r,z)$ can be calculated from the axial distribution of the same potential $V(z)$ by the following power series expansion [7]:

$$V(R_p, z) = \sum_{k=0}^{\infty} \frac{(-1)^k}{(k!)^2} \left(\frac{R_p}{2}\right)^{2k} \frac{d^{2k} V(z)}{dz^{2k}} \quad (6)$$

where R_p is the radial height of the polepiece. Taking the first two terms of equation 6 under consideration, the equipotential surfaces (polepiece shapes) are given by the following formula:

$$R_p(z) = 2 \sqrt{\frac{(V_z - V_p)}{V_z''}} \quad (7)$$

where V_p is the value of the potential at the iron base of the polepiece. Eq. 7 has been applied on the two equivalent parts of the symmetrical field.

Results and Discussion

The effect of halfwidth W on the field distribution and its focal properties can be investigated by keeping the remaining two parameters constant at the following values $B_{max}=1T$ and $L=40mm$. The axial flux density B_z and the corresponding axial magnetic scalar potential V_z for each value of W are shown in fig. 2 and 3. It is clear that the area under the curve increases as long as W increases, i.e. the refractive power NI increases with the increase of the value of W . Since the excitation parameter $NI/V_r^{1/2}=25$ is kept constant the acceleration voltage V_r increases with respect to the increase of NI .

Fig. 4 shows the electron beam trajectory inside the magnetic field distribution for different values of the halfwidth ($W=1, 2, 3, 4, 5$ mm) when $B_{max}=1T$ and $L=40mm$ at $NI/V_r^{1/2}=20$ under zero magnification condition. It should be noted that the electron beam enters the magnetic field in the same height. Since the present investigation deals with determined the projector properties, the electron beam trajectory calculated with aid of the paraxial ray equation along the total length of the magnetic electron lens. From the figure, one can see that when the halfwidth w increases the refractive power of the magnetic field decreases for the electron beams, this means that when the halfwidth increases the lens excitation increases. Therefore, electron beam needed more acceleration voltage to penetrate field distribution for large halfwidth [6].

Fig. 5 shows the reconstruction procedure of the magnetic lens polepieces for different values of the halfwidth ($W=1, 2, 3, 4, 5$ mm) when $B_{max}=1T$ and $L=40mm$. It should be noted that the polepiece diameter D and the air gap width S are increased with the increase of the value of W . For high values of the halfwidth, the polepiece shape are very complex in design field, therefore, in order to neglect the manufacturing difficulties. Designer should be considered the lower values of the parameter W as possible as [1].

Fig. 6 represents the relationship between the projector focal length F_p with the excitation parameter $NI/V_r^{1/2}$. It is seen that the value of the projector focal length decreases with the

increase of the excitation parameter until reach the minimum value $((F_p)_{\min} = 0.440808, 0.88117, 1.321719, 1.762284, 2.202852 \text{ mm})$ for the mentioned W values taken under consideration. So, we seen that the values of the minimum projector focal length $(F_p)_{\min}$ for all the values of halfwidth produce at the same of excitation parameter $NI/V_r^{1/2} = 14.2$. Also, we saw that when the values of halfwidth increases the values of focal length increases, that's meaning when the values of halfwidth increases the area under the curve of field distribution increases [6].

Fig. 7 represents the relationship between the radial distortion coefficient and excitation parameter $NI/V_r^{1/2}$. It is seen that for each curve of the radial distortion coefficient has constant value at minimum excitation parameter and increases till reaches maximum value, then decreases until reaches zero approximately at excitation parameter $NI/V_r^{1/2} \approx 15$ and continue toward negative value with the increase of the excitation parameter. One can see that from the figure, when the halfwidth of the field increases the radial distortion coefficient D_r has small values. This means that the field distributions of small halfwidth have large values of the radial distortions [6]. It should be that the magnetic projector lenses in present work have no radial distortion at the excitation parameter in which the minimum projector focal length occurs for all W values. This means that these lenses have no radial distortion at the excitation parameter in which the maximum magnification occurs.

The radial distortion parameter Q_r as a function of the excitation parameter $NI/V_r^{1/2}$ for various values of the halfwidth is shown in fig. 8.

Fig. 9 represents the variation of the spiral distortion coefficient with the excitation parameter $NI/V_r^{1/2}$. It is seen that the values of spiral distortion coefficient increase rapidly at small values of the halfwidth with the increase of the excitation parameter. It should be mentioned that for the large values of the halfwidth of the field distribution the magnetic projector lens has small distortion. This behavior can be explained as the halfwidth increases the bore radius and, the air gap region of the reconstructed projector magnetic lenses are increasing.

Fig. 10 shows the variation of the spiral distortion parameter Q_s with the excitation parameter $NI/V_r^{1/2}$. The curves in the figure 10 have one minimum value equal $(Q_s)_{\min} = 0.893$ at excitation parameter extend from $(NI/V_r^{1/2} = 9.1)$ to $(NI/V_r^{1/2} = 9.7)$, this value less than unity $((Q_s)_{\min} = 1)$ is well known at symmetrical projector lenses [8].

The low value of spiral distortion parameter Q_s gives possible reduce the projector distance for the electron microscope and then get on the large projector angle, this leads to reduce the length tube of the electron microscope.

Fig. 11 represents the minimum value of focal length, radial distortion parameter and spiral distortion parameter, lens excitation NI and acceleration voltage V_r as a function of the halfwidth at constant maximum value of the flux density. The relationship between $(F_p)_{\min}$ and NI with W are linear. But, Q_r and Q_s are not effected by values of W because the value of maximum flux density is constant. The value of $(Q_r = 0.13)$ at $(NI/V_r^{1/2} = 15)$ and $(Q_s = 0.893)$ at $(NI/V_r^{1/2} = 9.1 \text{ to } 9.7)$. The variation of the accelerated voltage V_r with halfwidth W is shown in the same figure (11). It indicates that in order to increase the halfwidth W one should increase the acceleration voltage, but not linearly because the area under the curve increases with halfwidth increase.

References

1. Warid, H.H. (2006), Approximation of the Magnetic Field distribution for Objective Magnetic Lenses by Using Analytical Function"J.of College of Education, 3:360-381.

2. Hawkes, P.W. (1982). Magnetic Optical Synthesis and Optimization "PROCEEDINGS OF THE IEEE, 73:412-418.
3. Al-Obaidi, H. N. (1995), Determination of the design of magnetic electron lenses operated under preassigned magnification conditions"Ph.D. Thesis, University of Baghdad, Iraq.
4. Al-Batat, A. H. H. (1996), Inverse design of magnetic lenses using a defined magnetic field, M.Sc. Thesis, University of Mustansiriyah, Baghdad, Iraq.
5. Al-Kadumi, K.S. (2007). Computer-Aided-Design of Optimized Magnetic Electron Lenses M.Sc. Thesis, University of Mustansiriyah, Baghdad, Iraq.
6. Zangana, H. A. (2005). Using Gray's model as a target function in the inverse design of magnetic lenses M.Sc. Thesis, College of Education, The University of Mustansiriyah, Baghdad, Iraq.
7. Szilagy, M. (1984), Reconstruction of electrodes and polepieces from optimized axial field distributions of electron and ion optical systems, Appl. Phys. Lett. 45: 499-501.
8. Lambrakkis, E.; Marai, F.Z. and Mulvey, T., (1977). Correction of Spiral Distortion In the TEM"Development in Electron Microscopy and Analysis .Ed.D.I Misell (Inst.Phys.Conf.Sonf.Ser.NO.36: 35-38.

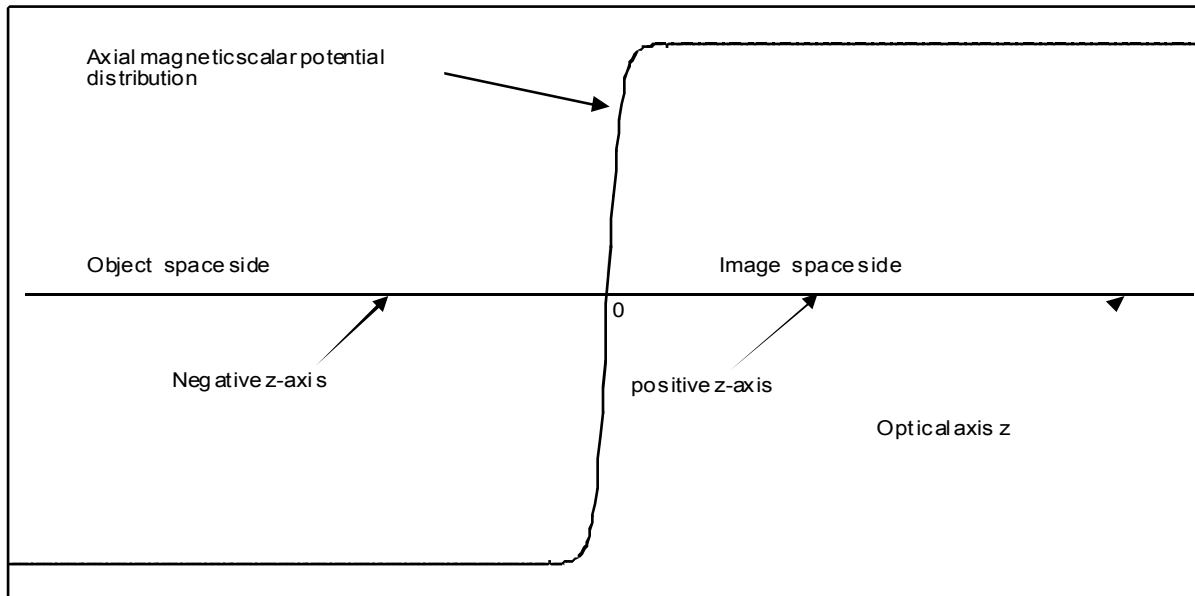


Fig.(1): The axial magnetic scalar potential distribution of symmetrical double polepiece magnetic lens.

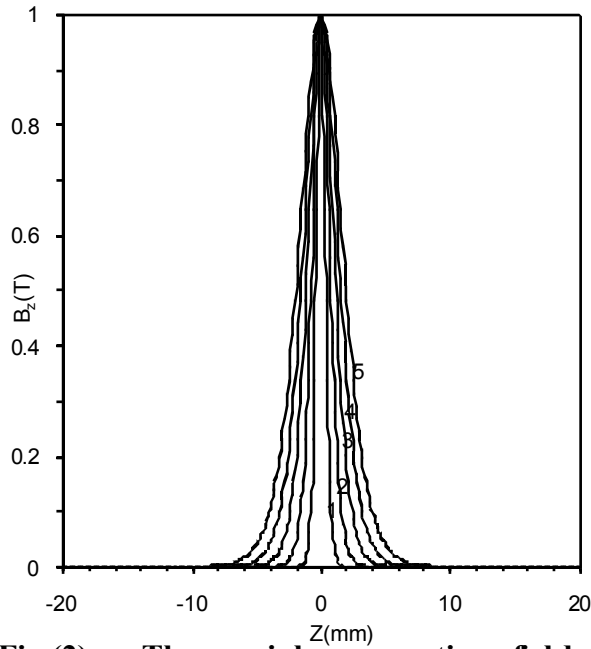


Fig.(2): The axial magnetic field distribution for different values of ($W=1, 2, 3,4,5$ mm) when $B_{max}=1T$ and $L=40mm$.

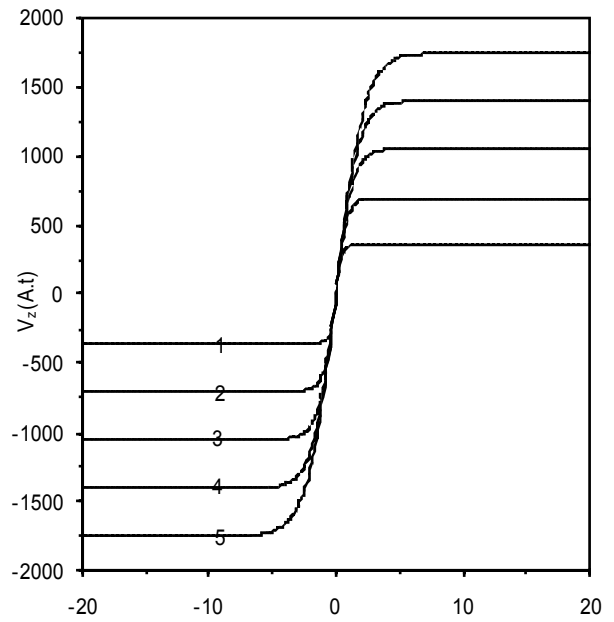


Fig.(3): The axial magnetic scalar potential distribution for the field plotted in fig. 2.

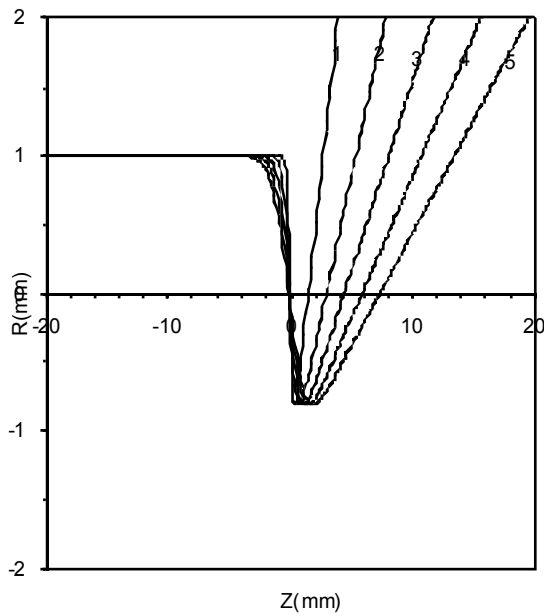


Fig. (4): Electron beam trajectory inside the magnetic field for different values of ($W=1, 2, 3, 4, 5$ mm) when $B_{max}=1T$ and $L=40$ mm at $NI/Vr^{1/2}=20$.

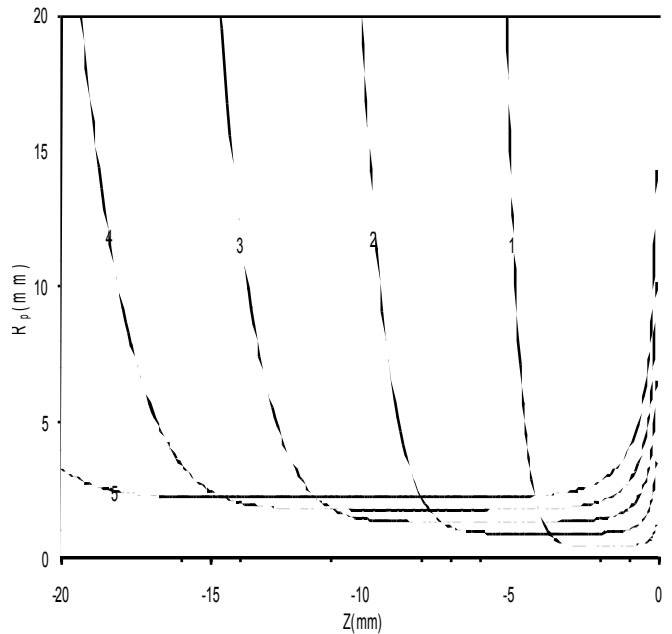


Fig. (5): Profile of polepieces for different values of ($W=1, 2, 3, 4, 5$ mm) when $B_{max}=1T$ and $L=40$ mm.

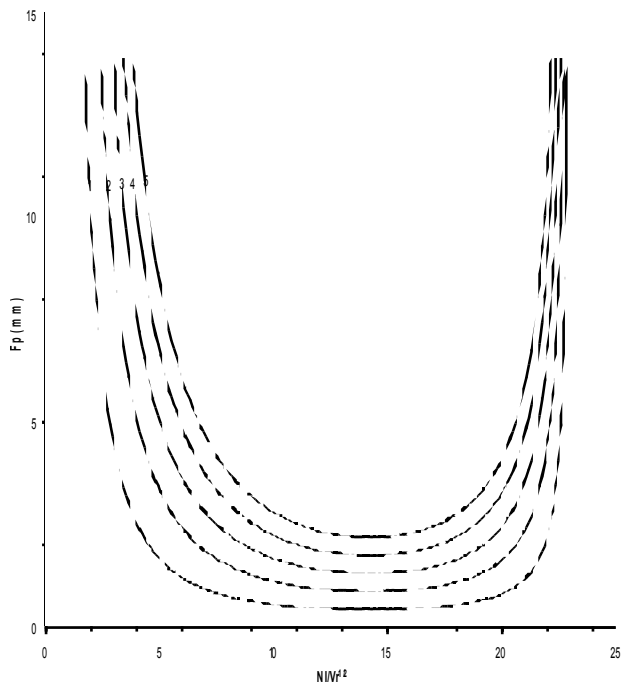


Fig. (6): The projector focal length against excitation parameter for different values of ($W=1, 2, 3, 4, 5$ mm) when $B_{max}=1T$ and $L=40mm$.

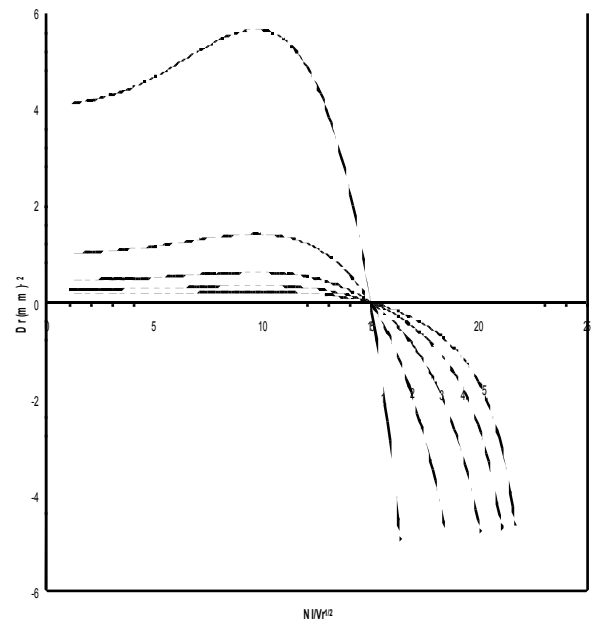


Fig. (7): The radial distortion coefficient against excitation parameter for different values of ($W=1, 2, 3, 4, 5$ mm) when $B_{max}=1T$ and $L=40mm$.

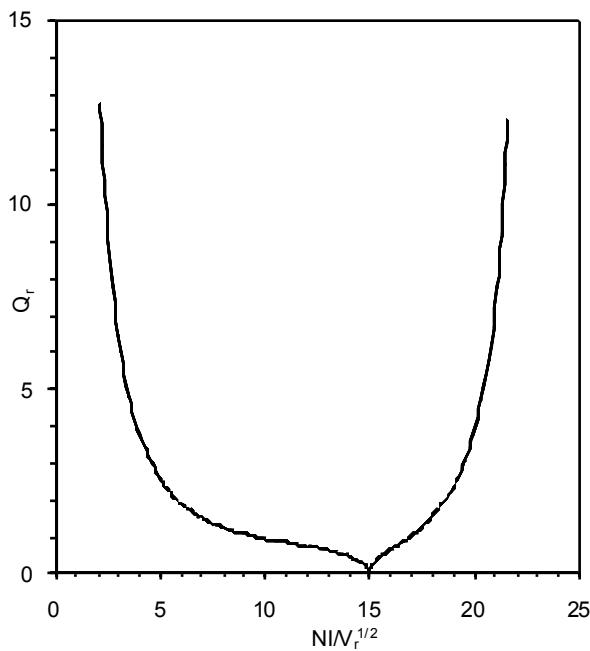


Fig. (8): Variation of the radial distortion parameter with the excitation parameter for different values of ($W=1, 2, 3, 4, 5$ mm) when $B_{max}=1T$ and $L=40mm$.

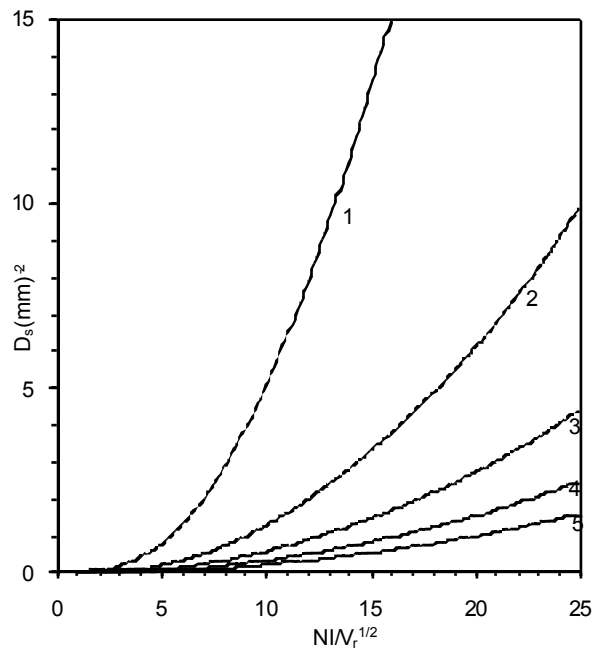


Fig. (9): The spiral distortion coefficient as a function of the excitation parameter for various values of ($W=1, 2, 3, 4, 5$ mm) when $B_{max}=1T$ and $L=40mm$.

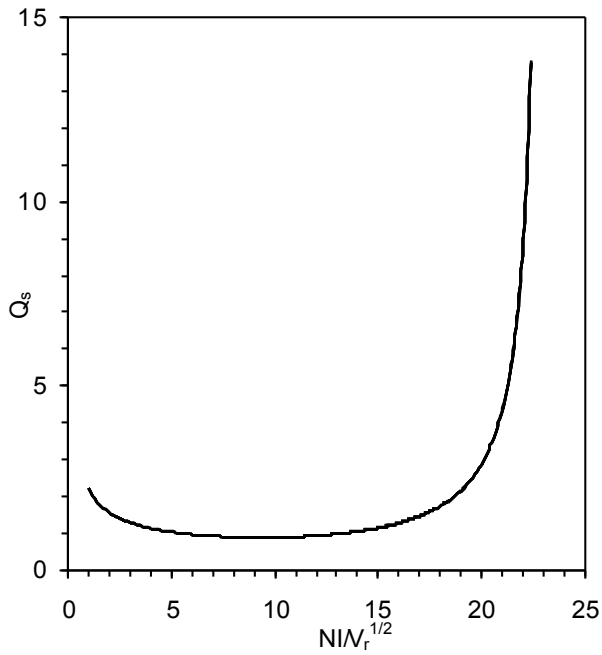


Fig. (10): Variation of the spiral distortion parameter Q_s with $NI/V_r^{1/2}$ for different value of W at $B_{max}=1T$ and $L=40mm$.

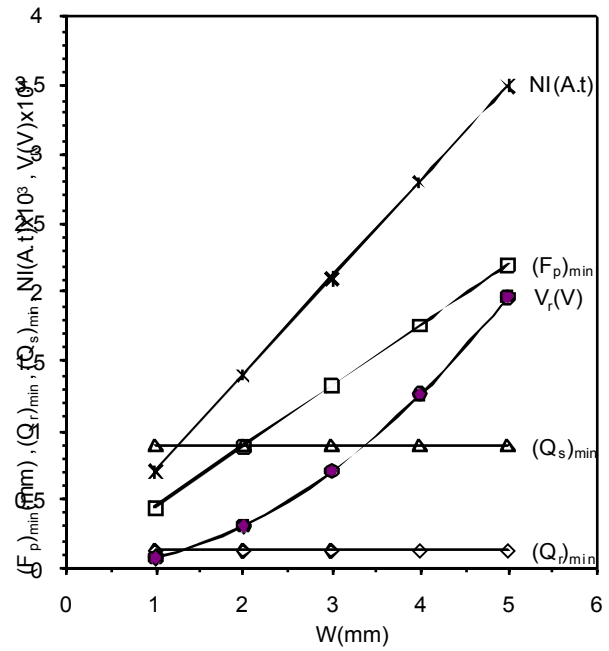


Fig. (11): The minimum projector focal length, spiral distortion parameter, radial distortion parameter, lens excitation NI and accelerated voltage V_r as a function of the halfwidth of the magnetic field at constant excitation

دراسة الخواص المسقطية لعدسات مغناطيسية باستعمال دالة تحليلية

علي هادي حسن البطاط، محمد جواد ياسين، ميادة منذر مجيد*

قسم الفيزياء، كلية التربية، الجامعة المستنصرية

*قسم الطب الحيوي، كلية هندسة الخوارزمي، جامعة بغداد

استلم البحث في 29 ايلول 2010

قبل البحث في 8 شباط 2011

الخلاصة

في هذا البحث أجريت دراسة تصف طريقة من طرائق التوليف الامثل للعدسات المغناطيسية . وقد تركز البحث على إيجاد التصميم العكسي للعدسات المغناطيسية ثنائية القطب المتناظرة التي حدّد توزيع مجالها المغناطيسي مسبقاً. وتمت الاستفادة من أنموذج التوزيع، حيث درس المجال عندما يكون عرض النصف متغيراً والقيمة العظمى لكثافة الفيض المغناطيسي ثابتة. تكمن أهمية هذا البحث تكمن في إمكانية الاستفادة من الطريقة التوليفية المتبعة وذلك بإيجاد تصميم أقطاب العدسة المغناطيسية الثنائية القطب المتناظرة التي لها خواص مسقطية مقبولة.

كلمات المفاتيح: بصريات الالكـتـرون، عدسات الكـتـرونية مغناطيسية

، تصميم عكسي للعدسات المغناطيسية ، امسلية العدسات المغناطيسية